Bioresource Technology 161 (2014) 149–154

Contents lists available at ScienceDirect

Bioresource Technology

journal homepage: www.elsevier.com/locate/biortech

Study of cellular development and intracellular lipid bodies accumulation in the thraustochytrid *Aurantiochytrium* sp. KRS101

Natarajan Velmurugan [a], Yesupatham Sathishkumar [b], Sung Sun Yim [a], Yang Soo Lee [b], Min S. Park [a,c], Ji Won Yang [a], Ki Jun Jeong [a,d,*]

[a] Department of Chemical and Biomolecular Engineering (BK21 Program), KAIST, Yuseong-gu, Daejeon 305-701, Republic of Korea
[b] Department of Forest Science and Technology, College of Agriculture and Life Sciences, Chonbuk National University, Jeonju, Republic of Korea
[c] Bioscience Division, Los Alamos National Laboratory, Los Alamos, NM, USA
[d] Institute for the BioCentury, KAIST, Daejeon, Republic of Korea

HIGHLIGHTS

- Structural correlation between cellular development and lipid body accumulation.
- HTP screening of thraustochytrid using FACS with different fluorescent dyes.
- Found that BODIPY 505/515 with less concentration of DMSO effective for FACS.
- Established a quantitative baseline for lipids accumulation and/or microalgal growth.

ARTICLE INFO

Article history:
Received 14 January 2014
Received in revised form 26 February 2014
Accepted 4 March 2014
Available online 14 March 2014

Keywords:
Aurantiochytrium sp.
TEM analysis
BODIPY 505/515
Nile Red
Fluorescence-activated cell sorting

ABSTRACT

Transmission electron, confocal microscopy and FACS in conjunction with two different lipophilic fluorescent dyes, BODIPY 505/515 and Nile Red were used to describe the cellular development and lipid bodies formation in *Aurantiochytrium* sp. KRS101. TEM results revealed that multi-cellular spores were appeared in sporangium during early-exponential phase, and spores were matured in mid-exponential phase followed by release of spores from sporangium in late-exponential phase. TEM and FACS analyses proved that lipid bodies appeared, developed and degenerated in mid-exponential, early- and late-stationary phases, respectively. The staining results in FACS indicate that BODIPY 505/515 is more effective for the vital staining of intracellular lipid bodies than Nile Red. FACS based single cell sorting also showed healthy growth for BODIPY 505/515 stained cells than Nile Red stained cells. In addition, a quantitative baseline was established either for cell growth and/or lipid accumulation based on cell count, fatty acid contents/composition, and sectional/confocal images of KRS101.

1. Introduction

Of the marine heterotrophs (Labyrinthulomycota), the group thraustochytrids has been recognized as a potential source of essential fatty acids for commercially valuable products such as biodiesel and DHA (Gupta et al., 2012; Shene et al., 2013). In the past few years, researchers reported on the useful oil accumulation in single-celled marine microbes such as fungal-like microorganisms (Labyrinthulomycetes) and green microalgae (Kobayashi et al., 2011; Matsuda et al., 2012). Several thraustochytrids have been screened to produce value-added products polyunsaturated fatty acids (PUFAs), carotenoid pigments, carbohydrates, proteins and several degrading enzymes (Arafiles et al., 2011; Raghukumar, 2008; Shene et al., 2010; Shimidzu et al. 1996). In thraustochytrids, major fatty acids synthesized in vivo are n-6 docosapentaenoic acid (DPA-C22:5), docosahexaenoic acid (DHA-C22:6), palmitic acid (C16), eicosapentaenoic acid (EPA-C20:5), and arachidonic acid (AA-C20:4) (Kobayashi et al., 2011). The DHA derived from marine microbes are potential alternative to the limited natural resources such as marine fish oil and have high oxidative stability and sustainability as a raw material (Wong et al., 2008). Microbial-derived palmitic acids are energy-rich compounds which can be converted to biodiesels (Goodson et al., 2011; Radakovits et al., 2010). Of the thraustochytrids, the genus *Aurantiochytrium* has been widely used as a single-cell microbe to study lipid bodies that

* Corresponding author at: Department of Chemical and Biomolecular Engineering (BK21 Program), KAIST, Yuseong-gu, Daejeon 305-701, Republic of Korea. Tel.: +82 42 350 3934; fax: +82 42 350 3910.
E-mail address: kjjeong@kaist.ac.kr (K.J. Jeong).

http://dx.doi.org/10.1016/j.biortech.2014.03.017
0960-8524/

contain docosahexaenoic acid and palmitic acids (Jakobsen et al., 2008). The fatty acids compositions of intracellular lipid bodies in *Aurantiochytrium* depend on the composition of nutrient medium and researchers altered it by using different compositions of the nutrient medium (Kim et al., 2013). But, the structural correlation between the cellular physiology, development and ultrastructure in relation with intracellular lipid accumulation are poorly documented in the genus *Aurantiochytrium*. Thus, it is necessary to conduct a comparative characterization of cellular development, ultrastructure, lipid content and composition of the genus *Aurantiochytrium*, this could help us to develop *Aurantiochytrium* sp. as a suitable microbe for microalgal biodiesel and value-added products research.

The physiological states of many single-celled microorganisms, including bacteria, fungi, yeast, microalgae and mammalian cells have been studied by flow cytometry (Davey and Kell, 1996). The epifluorescence technique has been most commonly used to detect thraustochytrids cells, such as in Damare and Raghukumar (2008) where they used the acriflavine direct detection (AfDD) technique to detect the thraustochytrids cells. However, detection of intracellular lipid bodies of Labyrinthulomycetes in combination with lipophilic fluorescent dye has not been well studied. Flow cytometry in combination with a suitable fluorescent dye offers a unique opportunity to rapidly isolate microalgae with high lipid content for the production of lipids and value-added products (Hyka et al., 2012). The lipophilic dyes such as Nile Red and BODIPY 505/515 have been most commonly used to detect intracellular lipid bodies of green microalgae (Cooper et al., 2010; Doan and Obbard, 2011). However, the lipophilic dye Nile Red reported to be toxic to the microalgal strains while BODIPY 505/515 emerged as a vital stain for detection of intracellular lipids in microalgae (Govender et al., 2012; Velmurugan et al., 2013). Few marine green microalgae have been isolated using flow cytometry in combination BODIPY 505/515 (Pereira et al., 2011). In addition to lipid specific fluorescent dyes, several fluorescent dyes and probes are commercially available, and can be used for cell component-specific labeling (Czechowska et al., 2008; Hyka et al., 2012). Fluorescent dye BODIPY 505/515 in combination with FACS allows single cell level isolation and regeneration of microalgal strains that possesses high lipid content and single cell isolation can be used to study single cell genomics (Velmurugan et al., 2013). If single cell genomics can be incorporated with the metabolic activity of an algal cell, it may be possible to metabolically engineer microalgae for high lipid and biomass production.

Here, a complete characterization of the thraustochytrid *Aurantiochytrium* sp. KRS101 with regard to its cell development, ultrastructure and lipid accumulation is presented. Specifically, a correlation between cell development, differentiation and accumulation and composition of intracellular lipid bodies of *Aurantiochytrium* sp. KRS101 was obtained. Furthermore, FACS in combination with two different lipophilic dyes Nile Red and BODIPY 505/515 were tested for the screening, isolation, and culture of a single cell of *Aurantiochytrium* sp. KRS 101.

2. Methods

2.1. Strains and culturing conditions

Aurantiochytrium sp. KRS101 kindly provided by Korea Research Institute of Bioscience and Bioengineering (Kim et al., 2013) was used in this study. The cells were stored in 25% (v/v) glycerol at −80 °C. The cells were grown in nutrient medium consisting of 60 g/L glucose, 10 g/L yeast extract, 9 g/L KH_2PO_4, 15 g/L sea salt, and 10 mg/L tetracycline. Cultures were maintained at 25 °C with an agitation speed of 100 rpm. Samples for analysis were taken at different intervals, including 0 h (samples were taken immediately after re-suspension). Optical density (OD) was measured by UV spectrophotometer (Beckman-Coulter DU 730 Life Science, CA) and cell counts were measured by haemocytometer (Neubauer-improved bright line, Marienfeld, Lauda-Konigshofen, Germany).

2.2. Nile Red and BODIPY staining

Nile Red staining of intracellular lipid bodies in *Aurantiochytrium* sp. was done as follows. Glycerol (Sigma Aldrich, St. Louis, MO) was added to the microalgae suspension to a final concentration of 0.1 g ml^{-1} and stored in a dark condition. Five microliters of Nile Red (9-(diethyl amino) benzo[a]phenoxazin-5(5H)-one, Sigma Aldrich, St. Louis, MO) stock solution (0.4 mg ml^{-1}) was added to 3 ml of the algal-glycerol suspension which was then gently shaken for 1 min. Samples were then incubated in darkness for 5–10 min at room temperature, and then samples were directly used for FACS and microscopic analyses.

BODIPY 505/515 (4,4-difluoro-1,3,5,7-tetramethyl-4-bora-3a,4a-diaza-s-indacen), was purchased from Sigma Aldrich. BODIPY 505/515 staining was performed as reported previously (Velmurugan et al., 2013). A 5 mM BODIPY 505/515 stock was prepared by dissolving in dimethyl sulfoxide (DMSO, Sigma Aldrich, St. Louis, MO) and stored in the dark. For efficient staining of the intracellular lipid bodies in *Aurantiochytrium* sp., an aliquot of 0.2% DMSO (vol/vol) was added to the microalgal suspension. Two microliter of BODIPY 505/515 solution was added into the l ml of algal-DMSO suspension and gently shaken for 1 min. Samples were then incubated in darkness for 5–10 min at room temperature, and then the samples were directly used for FACS and microscopic analyses.

2.3. Flow cytometric analysis and cell sorting

High speed flow cytometer, MoFlo XDP (Beckman Coulter, Fullerton, CA) was used for the analysis of cell staining and cell sorting. The fluorescence reading was performed upon the excitation of 488 nm argon laser. The emission signal was measured in two channels upon excitation of 488 nm argon laser. In details, FL1 channel centered at 530/40 nm, and FL2 channel centered at 580/30 nm. The samples mean fluorescence intensity values and images were recorded from the FACS analysis using SUMMIT Software Version 5.2. The FACS settings of all channels were the same for all sorting procedures. Coulter Isoton II Diluent fluid (Beckman Coulter, Bera, CA) was used in all experiments as flow cytometry sheath fluid. Single cell sorting was carried out using single cell sort precision mode, with a 70 μm nozzle. Single cells were sorted directly into wells of deep-96-well plates containing 1 ml of above mentioned medium. After cell sorting, plates were incubated for 5 days, in a shaking rotator under the same growth conditions as described above. Single cell growth was monitored every day and cultures were maintained until the visible healthy algal growth was achieved from a single sorted cell. In order to assess the growth stability of a sorted single cell and contamination rate, 10 μl of liquid portion from wells was observed until 5 day using light microscope to monitor the bacterial and fungal contamination (Hyka et al., 2012; Velmurugan et al., 2013).

2.4. Microscopic determination of lipids in microalgal cells using different fluorescent dyes

Laser scanning confocal microscope (Eclipse C1si, Nikon, Japan) with the excitation at 488 nm and the emission at 570–590 nm was used for selectively detecting microalgal lipid bodies in *Aurantiochytrium* sp. (Cooper et al., 2010).

2.5. Transmission electron microscopy

For intracellular analysis, 12, 24, 48, 72, 96 and 120 h cultures of *Aurantiochytrium* sp. grown under the conditions mentioned as above were used. Primary fixation was done with 2.5% glutaraldehyde (Daejung Chemicals, Gyonggi-do, Korea), 2% paraformaldehyde (EMS, Hatfield, PA), 0.25 M sucrose (Daejung Chemicals, Gyonggi-do, Korea) buffered with 0.1 M sodium cacodylate pH 7.2 (Sigma Aldrich, St. Louis, MO) for 5 h at 4 °C. The post fixation was done with 1% osmium tetroxide (Tedpella, Redding, CA) in 0.1 M sodium cacodylate buffer pH 7.2 for 2 h at 4 °C. Samples briefly washed with distilled water at room temperature. Samples were dehydrated with graded ethanol series (30%, 40%, 50%, 60%, 70%, 80%, 90%, 95% and 100%). Transition was done with 100% propylene oxide (EMS, Hatfield, PA). Infiltration was done with Embed812 resin overnight at 70 rpm using Peneteron (Sunkay Laboratories Inc., Japan) and allowed to polymerize at 70 °C for 48 h. Sections of 80 nm thickness were taken using Leica UCT ultramicrotome (Leica Mikrosysteme GmbH, Austria) and collected on copper grid followed by double staining with 2% uranyl acetate (EMS, Hatfield, PA). Then, all sections were stained with Reynold's lead citrate (EMS, Hatfield, PA) and examined on a transmission electron microscope (Hitachi H7650, Tokyo, Japan) (Modified method of Wong et al., 2008).

2.6. Total lipid and fatty acid analysis

The total lipids were extracted from the 10 mg of lyophilized biomass with chloroform–methanol (2:1 v/v) solvent mixture similar to the Folch's method (Folch et al., 1957). Fatty acid methyl esters (FAMEs) were produced from the extracted lipid by transesterification reaction. Briefly, methanol was added to the extracted lipids with sulfuric acid as a catalyst and transesterification reaction was allowed to occur at 100 °C for 10 min. After reaction, 1 ml of deionized water was added and the organic phase was separated from water phase by centrifugation at 4,000 rpm for 10 min. One ml of chloroform containing 0.5 mg of a C19:0 fatty acid (nonadecanoic acid) was added to each tube as an internal standard. The FAMEs in organic phase were analyzed by gas chromatography (HP5890, Agilent) with a flame ionized detector (FID) and INNOWAX capillary column (Agilent, USA, 30 m × 0.32 mm × 0.5 μm).

2.7. Statistical analysis

Triplicates of samples were maintained throughout the experiments. Statistical analyses were performed using SigmaPlot 10.0 software (Systat Software Inc., Chicago, IL). The results were expressed as means ± SD (standard deviation) of triplicate experiments.

3. Results and discussion

3.1. Physiological behavior and ultrastructure of Aurantiochytrium sp. KRS101

To obtain healthy growth of *Aurantiochytrium* sp. KRS101, the seed cultures were obtained from late log phase. The initial seed cultures for inoculum were maintained around $\sim 2.0 \times 10^4$ cells ml^{-1}. The growth rates of *Aurantiochytrium* sp. KRS101 were measured and shown in Fig. 1. The *Aurantiochytrium* sp. KRS101 was found to have a lengthy exponential growth phase that started from 12 h and ended in 72 h. The strain reached the stationary phase by 96 h and stabilized in 120 h. It has been reported that *Aurantiochytrium mangrovei* MP2 which shared structural similarity with *Aurantiochytrium* sp. KRS101, was easily ruptured under freshwater, resulting in a release of cytoplasm from the cells (Wong et al., 2008). However, with the supplement of high concentration of nitrogen and carbon sources, the cell rupture was significantly reduced in *Aurantiochytrium* sp. KRS101 (Kim et al., 2013). Thus, it is conceivable that, *Aurantiochytrium* sp. KRS101 grows fast using high quantity of nutrients available in the medium, without cell rupture, and attain stationary level after exhaustion of available nutrients in the medium.

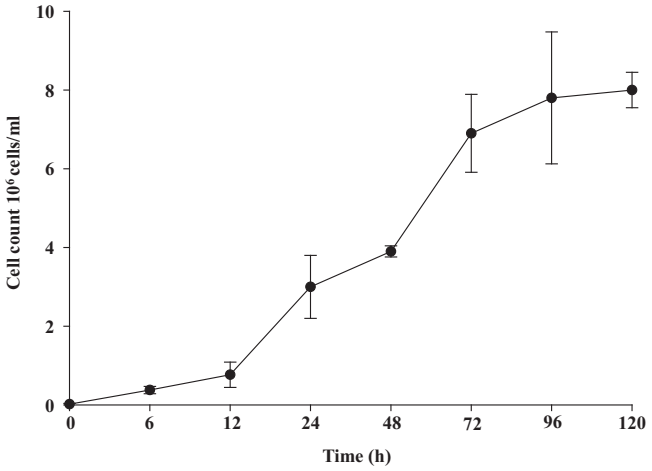

Fig. 1. Growth curve (cell count) for *Aurantiochytrium* sp. KRS101. Each data point represents three replicates.

Ultra structural correlation of lipid body formation have been extensively studied in the green algae *Chlamydomonas reinhardtii* and oleaginous fungus *Mortierella ramanniana* but analogous research in Labyrintulomycota including *Aurantiochytrium* sp. has yet to be undertaken (Goodson et al., 2011; Kamisaka et al., 1999; Gupta et al., 2012). The ultrastructure study with TEM analysis can illustrate the correlation between cellular growth and lipid body formation. During the culture period from lag phase (12 h) to late-stationary phase (120 h) (Fig. 1), we successfully observed that cells became heterogeneous in size and lipid bodies content increased gradually to those of lag phase cells (Table 1 and SI. F. 1–3). Nucleus, mitochondria, golgi bodies, small and large size vacuoles were clearly observed in both lag (12 h) and early-exponential phase (24 h) cells (SI. F. 1 and F. 2a, respectively), while those were not clearly observed in stationary phase cells. In early-exponential phase (24 h), mature lipid bodies were appeared and multi-cellular sporangiums were also appeared (SI. F. 2a and b). In this phase, we observed average appearance of 4–6 multi-cellular sporangiums per *Aurantiochytriu*m cell. In the mid-exponential phase (48 h), well-developed multi-cellular sporangiums were clearly observed (SI. F. 2c and d). But, in this phase, the outer layer of multi-layered membrane seems to be weaken and disconnected which cause the disruption of multi-layered outer membrane (SI. F. 2d). Very clear and high-level separations of young sporangiums were observed in late-exponential phase (72 h) (SI. F. 3a and b). Very interestingly, the early-stationary phase (96 h) cells showed large size and high quantity of lipid bodies (SI. F. 3c), those lipid bodies found to be more electron dense than early growth phases. It suggested that those lipid bodies have higher levels of unsaturated fatty acids than saturated fatty acids, because for staining the cells, we used osmium tetroxide which binds double bonds of unsaturated fatty acids (Wong et al., 2008; Bozzola and Russell, 1999). It is in correlation with our GC data that predominant species of lipid bodies are DHA and palmitic acid (Table 1). During late-stationary phase (120 h), disordered organelles and autophagosomes were observed and it suggested the malformation of the cells (SI. F. 3d). It has been

Table 1
GC quantification of FAME content of strains of *Aurantiochytrium* sp. KRS101 at different cell growth phases.

Growth phases	Total lipid (%)[a]	Fatty acid composition[b]				
		C14:0	C14:1	C16:0 (PA)	C18:0	C22:6n3 (DHA)
Lag phase (12 h)	10.4 ± 0.02	0.003	0.02	0.41	0.01	0.41
Early-exponential phase (24 h)	10.9 ± 0.3	0.003	0.03	0.5	0.02	0.51
Mid-exponential phase (48 h)	13.2 ± 0.2	0.04	0.002	0.53	0.01	0.53
Late-exponential phase (72 h)	18.5 ± 0.23	0.03	0.002	0.5	0.01	0.7
Early-stationary phase (96 h)	45.8 ± 0.33	0.3	0.007	2.6	0.1	1.9
Late-stationary phase (120 h)	50.5 ± 0.3	0.2	0.004	3.5	0.1	2.23

[a] All data are expressed as mean ± SD of triplicate experiments.
[b] All data are expressed as mean quantity of triplicate experiments.

noted that no sub-cellular sporangiums were released in the late-stationary phase suggesting that those cells are metabolically inactive than earlier growth phase cells, although they were still live in condition.

3.2. Comparison of the intracellular lipid content of Aurantiochytrium sp. by BODIPY 505/515 and Nile Red staining

One of the objectives of the present work was to compare the effectiveness of Nile Red and BODIPY 505/515 dyes to stain intracellular lipid bodies of Labyrinthulomycetes for flow cytometry-based screening and single cells sorting. For this purpose, first, the intracellular lipid accumulations in *Aurantiochytrium* sp. were analyzed by confocal microscope in combination with BODIPY 505/515 and Nile Red fluorescent dyes. So far, the evaluation of intracellular lipid bodies of Labyrinthulomycetes by lipophilic fluorescent dyes is scarce. Recently, the lipid bodies in thraustochytrid were stained using Nile Red but evaluation of efficiency had not been studied (Sakaguchi et al., 2012), while BODIPY 505/515 staining has not been reported yet. The lipophilic fluorescent dyes, Nile Red and BODIPY 505/515 have been used for the measurement of lipid contents in green microalgae and cyanobacteria (Govender et al., 2012; Velmurugan et al., 2013). The intracellular lipid droplets adsorb Nile Red and BODIPY 505/515 via a penetration and diffusion trap mechanism, respectively (Cooper et al., 2010). Different carrier solvents, acetone, glycerol and DMSO have been used for Nile Red to across the microalgal cell membrane (Cooksey et al., 1987; Doan and Obbard, 2011). However, higher quantities of acetone and DMSO inhibit algal cell growth (Doan and Obbard, 2011). The cell viability is an important point to be considered since one of the major aims of this study was to sort single thraustochytrid cells with high lipid content and recover those cells for further cultivation. Thus, the glycerol-based Nile Red staining selected for these studies.

Confocal microscopy images of Nile Red stained *Aurantiochytrium* sp. shown in SI. F. 4a and b. It is seen clearly that glycerol efficiently assisted Nile Red to penetrate the cell wall of *Aurantiochytrium* sp. and bind to lipid bodies emitting strong reddish fluorescence. These results regarding Nile Red staining of *Aurantiochytrium* sp. were consistent with the results reported by Sakaguchi et al. (2012). While significantly lower final concentrations of 0.02–0.2% of DMSO was used as a carrier solvent for BODIPY 505/515 staining in this study. Confocal microscopy images demonstrated that low concentrations of DMSO (0.02–0.2%) were effective to deliver BODIPY 505/515 into the *Aurantiochytrium* sp. (SI. F. 4c and d), while BODIPY 505/515 staining in a glycerol-algal suspension was not effective to stain lipid bodies (data not shown). The BODIPY 505/515 stained cells clearly distinguished the multi-cellular sporangium within the single cell (please note the white arrows in SI. F. 4c). This result indicates that the optimized DMSO–BODIPY composition highly efficient to transfer the BODIPY into the cells and BODIPY did not bind to multilayers of outer membranes and other cytoplasmic components in the multi-cellular sporangium within the single cell. While clearly distinguished multi-cellular sporangium have not found in Nile Red stained single cells, this also indicates the advantage of use of BODIPY staining over Nile Red staining. Suitability of significantly lower concentrations of DMSO for single cell sorting of *Aurantiochytrium* sp. detailed in single cell sorting section. Very clear bright green lipid droplets of *Aurantiochytrium* sp. were observed in confocal microscopy analysis and this suggests that the narrow emission spectrum of BODIPY 505/515 makes this dye more suitable than Nile Red for technical applications and staining with BODIPY 505/515 can provide a better resolved image than that obtained by Nile Red staining.

3.3. Determination of intracellular lipid contents in Aurantiochytrium sp. by FACS

After staining *Aurantiochytrium* sp. cells with Nile Red or BODIPY 505/515, the accumulation of intracellular lipid bodies in *Aurantiochytrium* sp. were also analyzed by FACS. Channels FL1 and FL2 were used for detection of fluorescent signals of BODIPY 505/515 and Nile Red, respectively. Fig. 2 presents a sequence of fluorescence histograms related to the different cell growth phases of *Aurantiochytrium* sp. KRS101, and the mean fluorescence intensity of each histogram is summarized in Table 2. In this comparison, results clearly showing that the relative fluorescence intensity for BODIPY 505/515 was greater than Nile Red fluorescence at all growth phases (Table 2 and Fig. 2). The mean fluorescence intensity of both Nile Red and BODIPY 505/515 stained *Aurantiochytrium* sp. cells gradually increased from the exponential to the stationary growth phase (Fig. 2 and Table 2), indicating the progressive accumulation of intracellular lipids as the cell cycle moved from the exponential phase to late-stationary phase. A peak fluorescence mean intensity of 1152.9 (a.u.) was obtained for Nile Red stained *Aurantiochytrium* at early-stationary phase (Table 2), this was relatively smaller value than mean fluorescence intensities of BODIPY stained cells obtained at same early-stationary phase. The mean fluorescent intensity from BODIPY stained *Aurantiochytrium* sp. was the highest (10332.01 a.u.) in the stationary phase (Table 2). Additionally, it observed that peaks between different cell growth phases were much clearly separated with BODIPY 505/515 staining than Nile Red staining (Fig. 2). These results clearly indicate the use of BODIPY 505/515 is more suitable than Nile Red for analysis of lipid production in *Aurantiochytrium* sp. The staining of lipids with BODIPY 505/515 was optimal to 0.2% DMSO as it did not affect cell viability and recovery at the concentration.

The fluorescent intensities obtained by FACS analysis were compared with lipid contents determined by GC analysis and we found both data have high correlation in most growth phases except for late-stationary phase (120 h) (Fig. 2 and Table 1). In both FACS and GC analyses, cells in exponential phase showed lower mean intensity values which were consistent with GC results, and these data indicate very slow accumulation of lipid in exponential

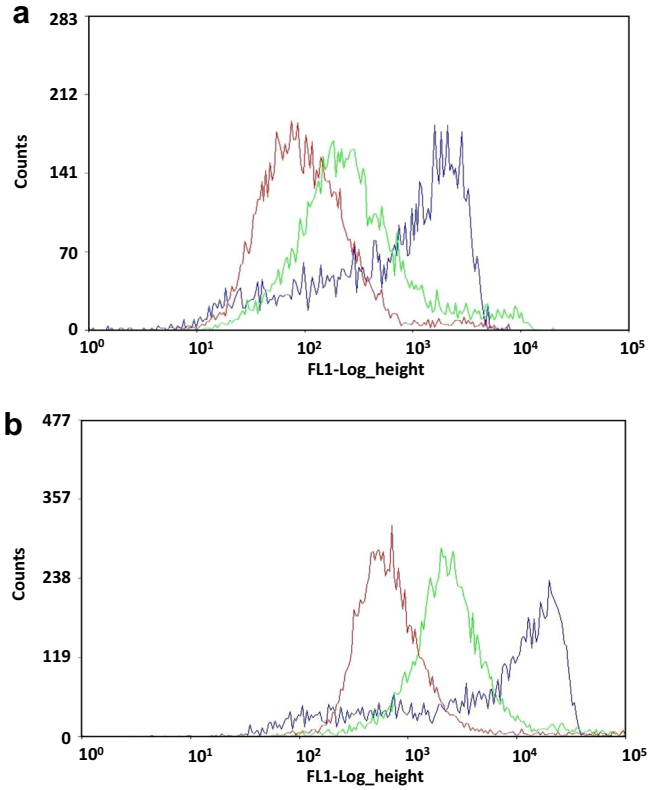

Fig. 2. Flow cytograms of Nile Red (a), and BODIPY 505/515 (b) stained *Aurantiochytrium* sp. KRS101. Red: early-exponential phase (24 h), green: mid-exponential phase (48 h), and blue: early-stationary phase (96 h). (For interpretation of the references to color in this figure legend, the reader is referred to the web version of this article.)

Table 2
Fluorescence intensities of Nile Red, and BODIPY 505/515 stained *Aurantiochytrium* sp. KRS101 at different cell growth phases.

Growth phases	Mean fluorescence intensity (a.u.)[a]	
	Nile Red stained (FL2 channel)	BODIPY stained (FL1 channel)
Lag phase (12 h)	157.94 ± 2.6	893.6 ± 0.6
Early-exponential phase (24 h)	183.84 ± 1.0	1800.4 ± 0.5
Mid-exponential phase (48 h)	193.43 ± 0.5	2499.52 ± 1.14
Late-exponential phase (72 h)	212.3 ± 2.1	3333.62 ± 1.4
Early-stationary phase (96 h)	1152.9 ± 3.1	10332.01 ± 1.5
Late-stationary phase (120 h)	763.9 ± 4.04	6234.41 ± 1.32

[a] All data are expressed as mean ± SD of triplicate experiments.

phase. Both analyses confirmed that the most significant accumulation of lipid was found in stationary phase. However, in FACS analysis, an unexpected result observed that cells at late-stationary phase exhibited significantly lower fluorescence intensity compared with early-stationary phase (Table 2). A possible reason for the decrease of signal intensities at late-stationary phase is that cells are disordered in the late-stationary phase and produced debris, further the fluorescent stained debris creates high noise during flow cytometry screening (data not shown) and showed relatively lower fluorescence than that of earlier growth phase.

3.4. Single cell sorting and viability analysis

In order to examine the effect of staining dyes on cell viability, *Aurantiochytrium* sp. cells stained with either Nile Red or BODIPY 505/515 were sorted by FACS and their cell growth were analyzed by cultivation. Using the single cell sort precision mode, the stained cells were separately sorted into 96-deep well plates containing 1 ml of nutrient medium mentioned in Methods. Approximately ~57% of the BODIPY 505/515 stained cells showed healthy growth while ~35% of the Nile Red stained cells showed healthy growth. In order to determine the contamination rate in the sorted cells, 10 μl of the liquid potion from a randomly selected well was continuously observed under light microscope and no bacterial or fungal contamination was observed. Different concentrations of DMSO (0.02–0.2%) in combination with BODIPY 505/515 stain was used to sort the single cells of *Aurantiochytrium* sp. and no significant difference in their post-sorting viability and recovery was found among the various concentrations of DMSO used. The results (no difference in post-sorting viability between unstained and BODIPY 505/515 stained cells, but reduction in post-sorting viability of Nile Red stained *Aurantiochytrium* cells) also indicate that BODIPY 505/515 is more efficient for single-cell sorting and regeneration of *Aurantiochytrium* sp. than Nile Red. Overall, the results indicating that FACS in combination with BODIPY 505/515 and minimum concentration of DMSO allows the sorting of individual cells possessing high lipid content successfully and used to seed new highly potent *Aurantiochytrium* sp. cultures. Post-sorting viability of microbial cells are affected by various reasons including toxic nature of dye, carrier substance used, fluid acceleration, electrical or mechanical shock and optical stress (Mutanda et al., 2011; Hyka et al., 2012). A fragile dinofagellate, *Karenia brevis* was reported for comparison of survival efficiency between FACS sorting and manual picking (Sinigalliano et al., 2009). The manual picking showed better efficiency than FACS sorting and this could be due to the fragility of algae that belong to this taxonomic group. Thus, the rate of successful post-sorting viability of single-cell of *Aurantiochytrium* sp. cells depends on taxonomic group, fluorescent dye, carrier solvent, instrument used and the optimization of recovery conditions of cell cultures is also required.

3.5. Fatty acid composition of Aurantiochytrium sp. by GC-FID analysis

To confirm the conclusions drawn from the FACS and TEM analysis, the fatty acid methyl esters (FAME) contents of *Aurantiochytrium* sp. KRS101 cells were quantified at different growth phases by gas chromatography. Fatty acid profiles of the *Aurantiochytrium* sp. KRS101 in the different growth phases are summarized in Table 1. The major fatty acid components observed in KRS101 cells were DHA (C22:6n3) and palmitic acid (C16). As shown in Table 1, the intracellular lipid content was periodically increased from lag phase to late-stationary phase. A significant shift in lipid content was observed from mid-exponential to late-stationary phase. Sequential increase of lipid content in different growth phases indicates the intergenerational stability of lipid levels in KRS101 cells. The presence of palmitic acid and DHA indicated the stable formation of fatty acid composition (Table 1). The DHA and palmitic acid contents are sequentially increased from lag- to late-stationary phase. Interestingly, a different alteration in fatty acid composition of KRS101 cells was observed during different growth phases. The palmitic acid (C16) content observed to be less than DHA (C22:6n3) until the end of the exponential phase but shifted to increase than DHA during stationary phase and attained highest level at late-stationary phase than DHA (Table 1). A study by Morita et al. (2006) reported that the content of palmitic acid in the 10-day old thraustochytrid *Schizochytrium limacinum* was higher than that of DHA content. However, observation of fatty acid composition of *Aurantiochytrium* not yet detailed at different growth phases.

3.6. The correlations between cellular distribution, FACS observations and FAME contents

A direct correlation between the morphological features, growth rates and intracellular lipid accumulation was investigated by using TEM, FACS analysis and FAME compositions. The exponential phase was started at 12 h and actively progressed until 72 h, during the exponential phase, cell growth increased from 0.7×10^6 to 6.9×10^6 cells ml^{-1}, while the active cell differentiations, formation and division of multi-cellular sporangiums within single cell and release of mature sporangium were positively observed by TEM analysis (SI. F. 1–3). FAME content results and FACS analysis showed the lipid accumulation was low in the exponential phase, but then increased in the stationary phase (Table 1 and Table 2), and TEM analysis also revealed the higher level of formation of intracellular lipid droplets. With regards to cell differentiation and lipid production, FACS analysis, FAME content results, TEM analysis and BODIPY 505/515 staining results positively correlated well during exponential and stationary phases. It was observed that formation of multi-cellular sporangiums was high and lipid accumulation was limited in exponential phase. However, cell division was reduced and lipid accumulation was increased in the stationary phase. It is due to the malfunctioning of cellular components and thus resulted collapse in metabolic pathways essential for proper functioning of various cell components. The correlation coefficient between Nile Red, BODIPY, and GC content was examined using samples at all growth phases and shown in SI. F.5. The correlation results were fit well from exponential phase till late-stationary phase.

4. Conclusions

The ultrastructure of *Aurantiochytrium* sp. KRS101 revealed the cellular development and lipid accumulation in combination of a high-throughput screening using FACS. Screening and sorting of KRS101 using FACS in combination of a low concentration of DMSO and BODIPY 505/515 was described. Significantly, morphological studies and FACS-BODIPY 505/515 staining results corresponded well with lipid accumulation in KRS101. A highly efficient screening methodology for the isolation high-lipid content cells from Labyrinthulomycota family using FACS in combination with BODIPY 505/515 was established. This study should facilitate the single cell genomics study of microalgal populations of Labyrinthulomycota family for the production of advanced biofuels.

Acknowledgements

This work was supported by the Advanced Biomass R&D Center (ABC) of Korea Grant funded by the Ministry of Science, ICT and Future Planning (MSIP) (ABC-2013-057282). N. Velmurugan was supported by the BK21 Post-Doctoral Research Fund and MSP was partially supported by Brain Pool Program of Korea.

Appendix A. Supplementary data

Supplementary data associated with this article can be found, in the online version, at http://dx.doi.org/10.1016/j.biortech.2014.03.017.

References

Arafiles, K.H.V., Alcantara, J.C.O., Cordero, P.R.F., Batoon, J.A.L., Galura, F.S., Leano, E.M., Dedeles, G.R., 2011. Cultural optimization of thraustochytrids for biomass and fatty acid production. Mycosphere 2, 521–531.

Bozzola, J.J., Russell, L.D., 1999. Electron Microscopy: Principles and Techniques for Biologists. Jones and Bartlett, Sudbury.

Cooksey, K.E., Guckert, J.B., Williams, S., Callis, P.R., 1987. Fluorometric determination of the neutral lipid content of microalgal cells using Nile Red. J. Microbiol. Methods 6, 333–345.

Cooper, M.S., Hardin, W.R., Petersen, T.W., Cattolico, R.A., 2010. Visualizing "green oil" in live algal cells. J. Biosci. Bioeng. 109, 198–201.

Czechowska, M., Johnson, D.R., van der Meer, J.R., 2008. Use of flow cytometric methods for single-cell analysis in environmental microbiology. Curr. Opin. Microbiol. 11, 205–212.

Damare, V., Raghukumar, S., 2008. Abundance of thraustochytrids and bacteria in the equatorial Indian Ocean, in relation to transparent exopolymeric particles (TEPs). FEMS Microbiol. Ecol. 65, 40–49.

Davey, H.M., Kell, D.B., 1996. Flow cytometry and cell sorting of heterogeneous microbial populations: the importance of single-cell analyses. Microbiol. Rev. 60, 641–696.

Doan, T.T.Y., Obbard, J.P., 2011. Improved Nile Red staining of *Nannochloropsis* sp. J. Appl. Phycol. 23, 895–901.

Folch, J., Lees, M., Stanley, G.H.S., 1957. A simple method for the isolation and purification of total lipids from animal tissues. J. Biol. Chem. 226, 497–509.

Goodson, C., Roth, R., Wang, Z.T., Goodenough, U., 2011. Structural correlates of cytoplasmic and chloroplast lipid body synthesis in *Chlamydomonas reinhardtii* and stimulation of lipid body production with acetate boost. Eukaryot. Cell 10, 1592–1606.

Govender, T., Ramanna, L., Rawat, I., Bux, F., 2012. BODIPY staining, an alternative to the Nile Red fluorescence method for the evaluation intracellular lipids in microalgae. Bioresour. Technol. 114, 507–511.

Gupta, A., Barrow, C.J., Puri, M., 2012. Omega-3 biotechnology: thraustochytrids as a novel source of omega-3 oils. Biotechnol. Adv., 1733–1745.

Hyka, P., Lickova, S., Pribyl, P., Melzoch, K., Kovar, K., 2012. Flow cytometry for the development of biotechnological processes with microalgae. Biotechnol. Adv. 31, 2–16.

Jakobsen, A.N., Aasen, I.M., Josefsen, K.D., Strom, A.R., 2008. Accumulation of docosahexaenoic acid-rich lipid in thraustochytrids *Aurantiochytrium* sp. strain T66: effects of N and P starvation and O_2 limitation. Appl. Microbiol. Biotechnol. 80, 297–306.

Kamisaka, Y., Noda, N., Sakai, T., Kawasaki, K., 1999. Lipid bodies and lipid body formation in an oleaginous fungus, *Mortierella ramanniana* var. *angulispora*. Biochim. Biophys. Acta 1438, 185–198.

Kim, K., Kim, E.J., Ryu, B.G., Park, S., Choi, Y.E., Yang, J.W., 2013. A novel fed-batch process based on the biology of *Aurantiochytrium* sp. KRS101 for the production of biodiesel and docosahexaenoic acid. Bioresour. Technol. 135, 269–274.

Kobayashi, T., Sakaguchi, K., Matsuda, T., Abe, E., Hama, Y., Hayashi, M., Honda, D., Okita, Y., Sugimoto, S., Okino, N., Ito, M., 2011. Increase of eicosapentaenoic acid in thraustochytrids through thraustochytrid ubiquitin promoter-driven expression of a fatty acid Δ5 desaturase gene. Appl. Environ. Microbiol. 77, 3870–3876.

Matsuda, T., Sakaguchi, K., Hamaguchi, R., Kobayashi, T., Abe, E., Hama, Y., Hayashi, M., Honda, D., Okita, Y., Sugimoto, S., Okino, N., Ito, M., 2012. Analysis of Δ12-fatty acid desaturase function revealed that two distinct pathways are active for the synthesis of PUFAs in *T. aureum* ATCC 34304. J. Lipid Res. 53, 1210–1223.

Morita, E., Kumon, Y., Nakahara, T., Kagiwada, S., Noguchi, T., 2006. Docosahexaenoic acid production and lipid-body formation in *Schizochytrium limacinum* SR21. Mar. Biotechnol. 8, 319–327.

Mutanda, T., Rames, D., Karthikeyan, S., Kumari, S., Anandraj, A., Bux, F., 2011. Bioprospecting for hyper-lipid producing microalgal strains for sustainable biofuel production. Bioresour. Technol. 102, 57–70.

Pereira, H., Barreira, L., Mozes, A., Florindo, C., Polo, C., Duarte, C.V., Custodio, L., Varela, J., 2011. Microplate-based high throughput screening procedure for the isolation of lipid-rich marine microalgae. Biotechnol. Biofuel. 4, 61–73.

Radakovits, R., Jinkers, R.E., Darzins, A., Posewityz, M.C., 2010. Genetic engineering of algae for enhanced biofuel production. Eukaryot. Cell 9, 486–501.

Raghukumar, S., 2008. Thraustochytrid marine protists: production of PUFAs and other emerging technologies. Mar. Biotechnol. 10, 631–640.

Sakaguchi, K., Matsuda, T., Kobayashi, T., Ohara, J.-I., Hamaguchi, R., Abe, E., Nagano, N., Hayashi, M., Ueda, M., Honda, D., Okita, Y., Taoka, Y., Sugimoto, S., Okino, N., Ito, M., 2012. Versatile transformation system that is applicable to both multiple transgene expression and gene targeting for thraustochytrids. Appl. Environ. Microbiol. 78, 3193–3202.

Shene, C., Leyton, A., Esparza, Y., Flores, L., Quilodran, B., Hinzpeter, I., Rubilar, M., 2010. Microbial oils and fatty acids: effect of carbon source on docosahexaenoic acid (C22:26 N-3, DHA) production by thraustochytrid strains. J. Soil Sci. Plant Nutr. 10, 207–216.

Shene, C., Leyton, A., Rubilar, M., Pinelo, M., Acevedo, F., Morales, E., 2013. Production of lipids and docosahexasaenoic acid (DHA) by a native *Thraustochytrium* strain. Eur. J. Lipid Sci. Technol. 115, 890–900.

Shimidzu, N., Goto, M., Wataku, W., 1996. Carotenoids as singlet oxygen quenchers in marine organisms. Fish Sci. 62, 134–137.

Sinigalliano, C.D., Winshell, J., Guerrero, M.A., Scorzetti, G., Fell, J.W., Eaton, R.W., Brand, L., Rein, K.S., 2009. Viable cell sorting of dinoflagellates by multiparametric flow cytometry. Phycologia 48, 249–257.

Velmurugan, N., Sung, M., Yim, S.S., Park, M.S., Yang, J.W., Jeong, K.J., 2013. Evaluation of intracellular lipid bodies in *Chlamydomonas reinhardtii* strains by flow cytometry. Bioresour. Technol. 138, 30–37.

Wong, M.K.M., Tsui, C.K.M., Au, D.W.T., Vrijmoed, L.L.P., 2008. Docosahexaenoic acid production and ultrastructure of the thraustochytrid *Aurantiochytrium mangrovei* MP2 under high glucose concentrations. Mycoscience 49, 266–270.